Journal of the Korean Society of Marine Environment & Safety
Research Paper
Vol. 26, No. 3, pp. 297-307, May 31, 2020, ISSN 1229-3431(Print) / ISSN 2287-3341(Online) https://doi.org/10.7837/kosomes.2020.26.3.297

Noise Analysis for Large Silencers of Ships and Off-shore Plants using Energy Flow Analysis

Tae-Gyoung Kim* · Jee-Hun Song**† · Suk-Yoon Hong***

* Ph.D. Candidate, Department of Naval Architecture and Ocean Engineering, Seoul National University, 1 Gwanak-ro, Seoul 08826, Korea
** Professor, Department of Naval Architecture and Ocean Engineering, Chonnam National University, 50 Daehak-ro, Yeosu 59626, Korea
*** Professor, Department of Naval Architecture and Ocean Engineering, Seoul National University, 1 Gwanak-ro, Seoul 08826, Korea

Abstract : *In the study, energy flow analysis is performed to predict the performance of silencers. To date, deterministic approaches such as finite element method have been widely used for silencer analysis. However, they have limitations in analyzing large structures and mid-high frequency ranges due to unreasonable computational costs and errors. However, silencers used for ships and off-shore plants are much larger than those used in other engineering fields. Hence, energy governing equation, which is significantly efficient for systems with high modal density, is solved for silencers in ships and off-shore plants. The silencer is divided into two different acoustic media, air and absorption materials. The discontinuity of energy density at interfaces is solved via hypersingular integrals for the 3-D modified Helmholtz equation to analyze multi-domain problems with the energy flow boundary element method. The method is verified by comparing the measurements and analysis results for ship silencers over mid-high frequency ranges. The comparisons confirm good agreement between the measurement and analysis results. We confirm that the applied analysis method is useful for large silencers in mid-high frequency ranges. With the proven procedures, energy flow analysis can be performed for various types of silencer used in ships and off-shore plants in the first stage of the design.*

Key Words : *Energy flow analysis, Multi-domain boundary element method, Hypersingular integral, Silences for ships, Mid-to-high frequency*

1. Introduction

Various types of silencers are used to mitigate noise from heating ventilation and air conditioning (HVAC) systems. Silencers are widely applied for various fields given recent improvements in quality of life. In the case of ships, the role of the silencer is extremely important because the HVAC system noise is directly transmitted into the cabin through a pipeline.

The noise generated from main engines, generators, propellers, pumps, air conditioning systems, etc., caused by ship and off-shore plants noise, is transmitted to each cabin in the form of air-borne and structural-borne sound. The air-borne sound is the noise transmitted through the air, and the noise transmitted in the form of vibration through the structure such as the hull wall and floor is called the structure-borne sound. There is a problem that the primary noise generated in the fan, the air conditioner, etc., and the secondary noise generated by the turbulence of the flow in the piping element are easily transmitted to the outlet through the piping due to the characteristics of the HVAC system connected to the piping components. For this reason, noise from HVAC systems is considered to be a major source of noise in cabins located away from main structures such as propellers and engines and airborne noise sources. Therefore, it is important to analyze and predict HVAC noise for the residential environment of passengers (Soares and Fricke, 2011; Vérin and Fremion, 2010; Holland and Wong, 1995)

Specifically, in special ships including cruise ships and offshore structures that are considered high value-added vessels, cabin noise standards are very strict, and there is a need to develop performance analysis technology for silencers to satisfy stringent noise standards. In contrast to other fields, given the larger duct size as shown in Fig. 1, we evaluate the noise reduction performance mainly by using the data provided by institutions such as the American Society of Heating, Refrigerating and Air Conditioning (ASHRAE) (Reynolds and Bledsoe, 1991) and the National Environmental Balancing Bureau (NEBB) (Bride and Bevirt, 1994). However, the range of sound absorption parameters is limited, and there is also a limitation that it is applied only to simple shapes with the aforementioned data.

The most commonly used methods for evaluating sound

* First Author : taegyoung@snu.ac.kr, 02-880-7331
† Corresponding Author : jhs@jnu.ac.kr, 061-659-7156

propagation through silencers include the finite element method (FEM) and boundary element method (BEM) (Ju at al., 2007; Mecdizadeh and Paraschivoiu, 2005; Ge and Zhang, 2006). In order to accurately perform a silencer analysis with FEM and BEM, it is necessary to adjust the mesh size based on wave length. An increase in the size of the structures and frequency range analysis leads to increases in the number of meshes required, and large structures and analysis at high frequency ranges lead to considerable increases in the time required for the analysis (Errico et al., 2019; Yao et al., 2019). Another approach involves theoretical analysis that considers the acoustic field as a truncated sum over the silencer eigenmodes (Ko, 1975; Kakoty and Roy, 2002). The method reduces the dimension of problems that aids in performing the analysis in a considerably faster manner than that using FEM and BEM model. However, although performance with the theoretical analysis for relatively small dissipative silencers is well quantified, the application of these methods to large silencers is still limited as higher-order modes emerge. It is observed that it is difficult to perform analyses for large sizes and high frequency ranges by using these techniques, specifically for ships and offshore industries in which ducts of diameters almost up to 1500 mm are installed (NORSOK STANDARD, 1999).

In order to solve such problems, energy-based methods are used. Statistical energy analysis (SEA) that is based on the diffuse field assumption was developed for high frequency analysis (Lyon and Dejong, 1995). The method provides a time- and space-averaged vibrational energy level in a subsystem, and thus it gives the total vibrational energy or alternatively yields the modal energy. Thus, SEA results in tremendous time savings although it only yields averaged energy values in the subsystem. Hence, it is impossible to determine the energy transfer path. Another promising energy-based approach that is termed energy flow analysis (EFA) was introduced by Belov and Rybak (1977). The SEA deals with global energies of finite subsystems while the energy flow method is based on local energy approach. The method was applied to and verified for various elastic media including beams, membranes, plates, and inner or outer acoustic fields (Nefske and Sung, 1989; Kwon et al., 2012).

EFA is approach for simulating high frequency of large-scale structures with a possibility to accurately solve the problem in the mid-high frequency range. It is based on deriving governing differential equations with respect to energy density variables, and can utilize BEM and FEM for solving them numerically (Bitsie, 1996; Besset et al. 2010; Kwon et al., 2011). Its advantage is the potential of modeling large structures, such as the ship structure, by relatively coarse mesh of finite elements. The EFA method is based on an energy equation analogous to the heat conduction equation in a steady state, of which the main quantities are the energy density and energy flow. This differential equation leads to a continuous analysis of structures or acoustic fields. Using this method, the spatial variations in the time- and locally space averaged energy density and energy transmission paths can be effectively predicted for a structure or for an acoustic field.

To estimate the silencer performance, BEM combined with EFA (energy flow boundary element method, EFBEM) is used. The analysis technique applies BEM to EFA that is considered a promising tool to overcome the limit of frequency of traditional BEM. In the study, packed silencers (specifically, for large sizes and mid–high frequency ranges) are analyzed using a multi-domain EFBEM. This is evaluated for a three-dimensional energy governing equation, and the energy density and intensity relation is obtained at interfaces between two different domains. In order to confirm the applicability of the approach to silencers, experiments are performed for packed silencers ranging in width from 0.2 m to 0.5 m, and the EFBEM results for the insertion loss (IL) are compared with the experimental data.

Table 1. Recent studies on large silencers

	Method	Maximum width (for a unit airway)	Characteristics
Kirby et al. (2014b)	Theoretical analysis	0.3 m	High Computational cost for large silencer
Kirby et al. (2014a)	FEM	0.2 m	Limitation in mid–high frequency
Wang and Wu (2016)	BEM	0.2032 m	Limitation in mid–high frequency
Shojaeefard and Talebitooti (2012)	SEA	0.2 m	Provide only average value
Williams et al. (2018)	Hybrid (Modal+FEM)	0.2 m	Limitation in mid–high frequency
Present study	EFA	0.5 m	Possible for - mid-high frequency - large silencer - energy distribution and transfer path visualization

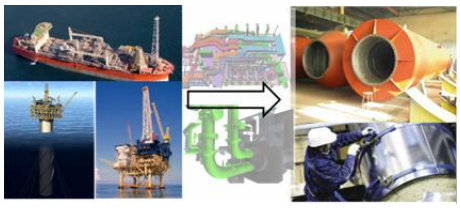

Fig. 1. Silencers for ship and off-shore plant.

2. Theory

2.1 Energy governing equation

When a steady state is considered, the acoustic power injected into a space of the medium is equal to the sum of the power flowing out through its boundary and the power dissipated in the medium. The steady state energy balance equation of a system is as follows:

$$\Pi_{diss} + \nabla \cdot \vec{I} = \Pi_{input}, \tag{1}$$

where Π_{diss} denotes the dissipated power owing to the damping, $\vec{I}$ denotes the intensity vector, i.e., the power transmitted through the boundary of the element, and Π_{input} denotes the input power. The energy loss caused by internal damping in the acoustic medium is expressed as follows:

$$< \Pi >_{diss} = \eta\omega < e >, \tag{2}$$

where the $< >$ brackets denote that the enclosed term is time-averaged over a period, η denotes the loss factor in the acoustic medium, ω denotes the circular frequency, and e denotes the total energy density. The damping loss factor depends on the frequency and reverberation time. The energy governing equation of energy flow analysis is obtained from the energy balance equation and energy loss equation and is expressed as follows:

$$-\frac{c_g^2}{\eta\omega}\nabla^2 e + \eta\omega e = \Pi_{\in put} \text{ and} \tag{3}$$

$$\vec{I} = -\frac{c_g^2}{\eta\omega}\nabla e, \tag{4}$$

where c_g denotes the group velocity in air. In the study, power input term Π_{input} in Eqn. (3) is omitted for purposes of simplicity because the term is not used to simulate the performance of the silencer. The equations are expressed as follows:

$$\nabla^2 e - k^2 e = 0 \text{ and} \tag{5}$$

$$\vec{\vec{I}} = \nabla e, \tag{6}$$

where k denotes a positive real number defined as $k = \frac{\eta\omega}{c_g^2}$. Equations (3), (4), (5), and (6) are compared, and $\vec{I}$ is transformed into $\vec{I} = -\frac{c_g^2}{\eta\omega}\vec{\vec{I}}$. Equation (5) is termed the modified Helmholtz equation, and the fundamental solution to three-dimensional problems is obtained as follows:

$$G(x,\xi) = \frac{1}{4\pi r} exp(-kr), r = |x - \xi| \tag{7}$$

where ξ denotes the collocation point, and x denotes the source point.

2.2 Hypersingular boundary integral equation

Equations (5) and (7) are used to derive the boundary integral equation by integrating over the interested domain Ω. If the input power term is excluded, the integral formulation for the EFA energy governing equation is derived as follows:

$$c(\xi)e(\xi) + \int_\Gamma e(x)F(x,\xi)ds = \int_\Gamma \vec{\vec{I}}(x)G(x,\xi)ds, \tag{8}$$

where the coefficient $c(\xi)$ is defined as $\alpha/2\pi$, and α denotes the internal angle at a collocation point ξ. When the smooth boundary of Γ is applied, $c(\xi)$ is expressed as follows:

$$c(\xi) = \begin{cases} 1 & \text{for } \xi \in \Omega \\ 0 & \text{for } \xi \notin \Omega. \\ 0.5 & \text{for } \xi \in \Gamma \end{cases} \tag{9}$$

Additionally, $F(x,\xi)$ is defined as follows:

$$F(x,\xi) = \frac{\partial G}{\partial n} = -\frac{e^{-kr}}{4\pi r^2}(1+kr)\frac{\partial r}{\partial n(x)}, \tag{10}$$

where $n(x)$ refers to a unit normal vector at a source pointing away from the domain of interest.

In order to analyze multi-domain EFBEM for silencers, the discontinuity problem of the energy density at interfaces as shown in Fig. 2 must be solved. Hypersingular integral equations are used to treat the problem. Hypersingular integrals were used in scattering problems (Wu, 1998) that are directly applied to boundary conditions for silencers (Wu and Wan, 1996). The important advantage of the approach is that it treats the pressure jump at interfaces between two domains by solving multi-domain problems without a special treatment for the discontinuity that occurs in various boundary conditions of the silencers. The discontinuity problem yielded by multi-domain EFBEM is solved with the approach.

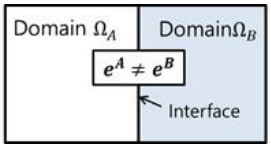

Fig. 2. Discontinuity problem for multi-domain EFBEM.

Hypersingular integral equations are obtained from the normal derivative of Eqn. (8) in terms of a collocation point ξ, and when a collocation point is located within the domain, it is expressed as follows:

$$\overrightarrow{I}(\xi) = \int_{\Gamma} e(x)F^{*}(x,\xi)ds = \int_{\Gamma} \overrightarrow{I}(x)G^{*}(x,\xi)ds, \quad (11)$$

where

$$F^{**}(x,\xi) = \frac{\partial^2 G(x,\xi)}{\partial n(x)\partial n(\xi)} = \frac{e^{-kr}}{4\pi r^3}[(3+3kr+k^2r^2)\frac{\partial r}{\partial n(x)}\frac{\partial r}{\partial n(\xi)} + (1+kr)n(x)n(\xi)] \text{ and} \quad (12)$$

$$G^{*}(x,\xi) = \frac{\partial G(x,\xi)}{\partial n(\xi)} = -\frac{e^{-kr}}{4\pi r^2}(1+kr)\frac{\partial r}{\partial n(\xi)}. \quad (13)$$

Equation (11) is valid for any point ξ within the domain. In order to calculate boundary values at interfaces between two domains, the case in which ξ is pushed on the boundary is considered, and Γ is divided into two parts as follows:

$$\overrightarrow{I}(\xi) + \int_{\triangle\Gamma} e(x)F^{*}(x,\xi)ds + \int_{\Gamma-\triangle\Gamma} e(x)F^{*}(x,\xi)ds = \int_{\triangle\Gamma} \overrightarrow{I}(x)G^{*}(x,\xi)ds + \int_{\Gamma-\triangle\Gamma} \overrightarrow{I}(x)G^{*}(x,\xi)ds, \quad (14)$$

where $\triangle\Gamma$ is a singular element.

To evaluate the hypersingular boundary integral, a special treatment is required in contrast to the case of weak and strong singularity. In the study, the singularity subtraction technique is used. The approach regularizes the hypersingular integrals by using the fundamental solution of the Laplace equation (Krishnasamy et al., 1990). The added-back term of its double normal derivative makes it a weakly singular problem as the strong singularities are canceled out in the subtraction. Singular element values in Eqn. (14) are expressed as follows:

$$F^{*}(x,\xi) = \int_{\triangle\Gamma} \frac{\partial^2 G(x,\xi)}{\partial n(x)\partial n(\xi)}ds = \int_{\triangle\Gamma} (\frac{\partial^2 G(x,\xi)}{\partial n(x)\partial n(\xi)} - \frac{\partial^2 \psi(x,\xi)}{\partial n(x)\partial n(\xi)})ds + \epsilon_{ijk}n_k(\xi)\oint_c \psi_{,j}dl_i \text{ and} \quad (15)$$

$$\int_{\triangle\Gamma} G^{*}(x,\xi)ds = \frac{\partial G(x,\xi)}{\partial n(\xi)} = 0.5, \quad (16)$$

where ψ denotes the Laplace fundamental solution, $\psi_{,j}$ denotes the partial derivative of ψ with respect to jth coordinate of x, ϵ_{ijk} is alternating symbol, C denotes the contour along the edge of the singular element $\triangle\Gamma$, $n_k(\xi)$ denotes the kth component of the unit normal vector at ξ, l_i denotes the ith coordinate of x, and the summation convention is used for repeated indices. The direction of the contour integration is selected such that the contour C and the normal vector n follow the right-hand rule. Therefore, we derive the hypersingular surface boundary integral equation by substituting Eqn. (15) and (16) into Eqn. (14) as follows:

$$e(\xi)[\int_{\triangle\Gamma} (\frac{\partial^2 G(x,\xi)}{\partial n(x)\partial n(\xi)} - \frac{\partial^2 \psi(x,\xi)}{\partial n(x)\partial n(\xi)})ds + \epsilon_{ijk}n_k(\xi)\oint_c \psi_{,j}dl_i] + \int_{\Gamma-\triangle\Gamma} e(x)F^{*}(x,\xi)ds = -0.5\overrightarrow{I}(\xi) + \int_{\Gamma-\triangle\Gamma} \overrightarrow{I}(x)G^{*}(x,\xi)ds. \quad (17)$$

2.3 Energy flow boundary integral equation for the multi domain problem

For two-domain problem, the energy governing differential equations are as follows:

$$\nabla^2 e - k_A e = 0 \text{ in air and} \tag{18}$$

$$\nabla^2 e - k_B e = 0 \text{ in the absorption materials} \tag{19}$$

where k_A and k_B denote the positive real number defined by $k_A = \frac{\eta_A \omega}{(c_g)_A}$ for air and $k_B = \frac{\eta_B \omega}{(c_g)_B}$ for the absorption material, respectively; η_A and $(c_g)_A$ denote the damping coefficient and group velocity of air, respectively, and η_B and $(c_g)_B$ denote the damping coefficient and group velocity of the absorption material, respectively.

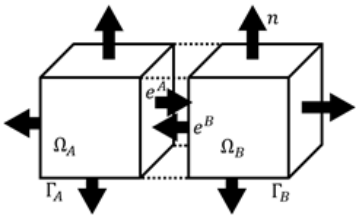

Fig. 3. Normal direction for multi-domain EFBEM

In the study, the experiment and simulation are performed for a model with a perforated panel between air and the absorption material, which is a widespread boundary condition used for the dissipate silencers. The boundary integral equations for every two domains are expressed as follows:

$$\int_{\Gamma_A+\Gamma_I} [e(x)F_A(x,\xi) - \vec{\vec{I}}(x)G_A(x,\xi)]ds = \begin{cases} -e(\xi) & \text{for} \xi \in \Omega_A \\ 0 & \text{for} \xi \in \Omega_A + \Gamma_B \\ -0.5(\xi) & \text{for} \xi \in \Gamma_A \end{cases} \text{ and} \tag{20}$$

$$\int_{\Gamma_B+\Gamma_I} [e(x)F_B(x,\xi) - \vec{\vec{I}}(x)G_B(x,\xi)]ds = \begin{cases} -e(\xi) & \text{for} \xi \in \Omega_B \\ 0 & \text{for} \xi \in \Omega_A + \Gamma_A \\ -0.5(\xi) & \text{for} \xi \in \Gamma_B \end{cases} \text{ and} \tag{21}$$

where notations A and B are used to express the related domain, namely A in air and B in the absorption material. Additionally, I denotes the interface between air and the absorption material. Normal vectors for Eqns. (20) and (21) point away from each domain Ω_A and Ω_B as shown in Fig. 3. With Eqns. (20) and (21), the number of equations for unknowns are insufficient, and thus additional equations are needed. The hypersingular surface integral equations are used for the supplement as follows:

$$\int_{\Gamma_A} [e(x)F_A^*(x,\xi) - \vec{\vec{I}}(x)G_A^*(x,\xi)]ds + \int_{\Gamma_I} [e(x)F_A^*(x,\xi) - \vec{\vec{I}}(x)G_A^*(x,\xi)]ds = -0.5\frac{\partial e}{\partial n}(\xi)$$

for $\xi \in \Gamma_I$ from the air side and (22)

$$\int_{\Gamma_B} [e(x)F_B^*(x,\xi) - \vec{\vec{I}}(x)G_B^*(x,\xi)]ds + \int_{\Gamma_I} [e(x)F_B^*(x,\xi) - \vec{\vec{I}}(x)G_B^*(x,\xi)]ds = -0.5\frac{\partial e}{\partial n}(\xi)$$

for $\xi \in \Gamma_I$ from the absorption material side (23)

Prior to summing up the integral equations, the discontinuity problem of energy density at the interface must be considered. In the study, the relationship between energy density and intensity at boundaries at every two domain is used to solve the problem. In a surface of the domain, energy density and intensity are expressed as follows:

$$\vec{\vec{I}} = \frac{1}{4}\alpha c_g e \tag{24}$$

By applying Eqn. (24) for every two domains and using them at interfaces, the relation equation is derived as follows:

$$e^A - e^B = \frac{4\vec{\vec{I}}}{\alpha}\left(\frac{1}{c_g^A} + \frac{1}{c_g^B}\right), \tag{25}$$

where upper indices indicate energy density values for air and the absorption material side at the interface, and the opposite sign is applied for intensity values of every two domain sides at the interface. Equation (25) is applicable for the summation of boundary integrals, Eqns. (20) and (21), and then unknown values are evaluated from the total surface boundary integral as follows:

$$\int_{\Gamma_A}[e(x)F_A-\vec{\vec{I}}(x)G_A]ds+\int_{\Gamma_B}[e(x)F_B-\vec{\vec{I}}(x)G_B]ds$$
$$+\int_{\Gamma_I}[e(x)^A(F_A+F_B-\vec{\vec{I}}(x)(G_A-G_B)$$
$$-\frac{4\vec{\vec{I}}}{\alpha}(\frac{1}{c_g^A}+\frac{1}{c_g^B})F_B]ds$$
$$=\begin{cases} e(\xi) & \text{for}\,\xi\in\Omega \\ 0.5e(\xi) & \\ & \text{for}\,\xi\in\Gamma_A\,\text{and}\,\Gamma_B \\ e(\xi)^A-\dfrac{2\vec{\vec{I}}(\xi)}{\alpha}(\dfrac{1}{c_g^A}+\dfrac{1}{c_g^B}) & \text{for}\,\xi\in\Gamma_I \end{cases} \quad (26)$$

$$\int_{\Gamma_A}[e(x)F_A^*-\vec{\vec{I}}(x)G_A^*]ds+\int_{\Gamma_B}[e(x)F_B^*-\vec{\vec{I}}(x)G_B^*]ds$$
$$+\int_{\Gamma_I}[e(x)^A(F_A^*+F_B^*-\vec{\vec{I}}(x)(G_A^*-G_B^*)$$
$$+\frac{4\vec{\vec{I}}}{\alpha}(\frac{1}{c_g^A}+\frac{1}{c_g^B})F_B^*]ds=\vec{I}(\xi)\ \text{for}\ \xi\in\Gamma_I \quad (27)$$

Here, repeated indices are omitted for purposes of simplicity. The absorption coefficient α must be obtained to apply Eqn. (25) to Eqns. (26) and (27), and this is evaluated from acoustic impedance at interfaces as follows:

$$\alpha=1-\left|\frac{Z_t+\rho c}{Z_t-\rho c}\right|^2, \quad (28)$$

where Z_t denotes the acoustic impedance for the summation of the perforated panel and the absorption material, ρ denotes the density of air, and c denotes the sound speed in air. In the next section, the derivation of Z_t is discussed in detail.

3. Validation for the performance of ship silencers

3.1 Experiment

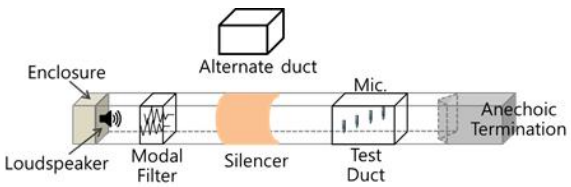

Fig. 4. Schematic of experimental set-up.

Simulation results from multi-domain EFBEM for a silencer are compared with measured data to verify the robustness of the proposed method. The measurement procedure is performed in accordance with the European Standard EN ISO 7235 (2003) and Fig. 4 illustrates the schematic of experimental set-up. The standard specifies methods for determining the IL and transmission loss of ducted silencers with and without airflow in frequency bands. It is applied to all types of silencers including silencers for ventilating air-conditioning systems, air intake, and exhaust of fuel gases and similar applications. Given the standard, a device was installed to measure the IL in the absence of flow. The device is mainly composed of a sound generator, a modal duct, silencer, or an alternate duct, a test duct for sound pressure measurement, and anechoic termination. Sound pressure is obtained by averaging the measured values from the five microphones installed in the test duct located downstream of the silencer by considering the difference in sound pressure based on the presence of the higher mode. Noise measurements were performed using BSWA MPA 416 microphone located in the end of ducts. Reliable frequency for a microphone ranged from 20 Hz to 20 kHz. Recordings were analyzed using NI sound and vibration software.

Flow is absent, and thus the anechoic termination was used as an end condition. Furthermore, the minimum length of each duct in the experimental setup is limited by the minimum interest frequency of 63 Hz, and the total length of the device is approximately 15 m to satisfy the requirement. Additionally, ISO 7235 specifies the installation of a modal filter and that a modal filter should exhibit an axial sound pressure reduction capability exceeding 3 dB in the lower frequency range that the cut-off frequency and exceeding 5 dB in the higher frequency range. The modal filter is installed between the speaker and the upper duct to suppress the transmission of the higher order mode generated by the speaker.

In the experiment, rectangular silencers are used, and in width and height are 0.2, 0.3, 0.4 and 0.5 m. The silencers are composed of absorption material and perforated steel. Mineral wool is used as the material, and it is separated from the airway in the silencer by a sheet of perforated steel.

3.2 Simulation

For a silencer as shown in Fig. 5 acoustic waves are mainly attenuated in the absorption material owing to viscous and thermal dissipation, and thus it is necessary to acquire information on the property of the absorption materials and to understand its relation

to a perforated panel to perform the analysis of the baffle silencers. In the case of energy-based analysis, absorption coefficients play an important role in reflecting the effect of a silencer, and they are derived from the empirical formula for absorption materials and perforated panels.

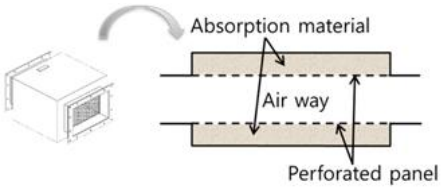

Fig. 5. Silencer model plane.

In the present study, the complex numbers of characteristic impedance and wavenumber are obtained from the bulk acoustic properties experimentally determined by Delany and Bazley (1970) to consider the dissipation of waves through the absorbing material. An impedance tube is used as shown in Fig. 6. Thus, the characteristic impedance $\tilde{Z}$ and wavenumber $\tilde{k}$ for rock wool are given as follows (Williams et al., 2014):

$$\tilde{Z}= \rho c[1+0.132(\frac{\rho f}{R_f})^{-0.54}]+i[-0.159(\frac{\rho f}{R_f})^{-0.533}] \quad (29)$$

$$\tilde{k}= k_0[1+0.086(\frac{\rho f}{R_f})^{-0.70}]+i[-0.175(\frac{\rho f}{R_f})^{-0.59}], \quad (30)$$

where f denotes frequency, ρ denotes density and R_f denotes the flow resistivity of the porous material determined from experiment. In order to measure the flow resistivity of the porous material in the reference, ISO 29053 (1993) is used.

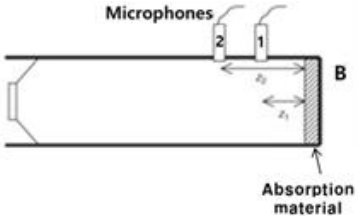

Fig. 6 Impedance tube.

For acoustic impedance of the perforated panel installed between airway and the absorbing material, the semi-empirical model proposed by Selamet et al. (2001) is used. The model is proposed to improve the method given by Kirby and Cummings (1998) that fails if it is applied to dissipative silencers with an erroneous transmission loss prediction due to an overestimated perforation impedance. The interaction among holes is considered, and the acoustic impedance of the perforated panel in the presence of absorbing material is given as follows:

$$\zeta_p = \frac{0.006+ik_0(t_w+0.375(1+\frac{\tilde{Z}}{\rho c}\frac{\tilde{k}}{k_0})d_h)}{\Phi}. \quad (31)$$

Here, t_w denotes the thickness of the perforated screen, d_h denotes the hole diameter, and Φ denotes the open area porosity of the perforated panel.

Predictions obtained from the bulk acoustic properties and the acoustic impedance of perforated panel above are used to derive absorption coefficients of the examined silencers. Total acoustic impedance of the silencers is considered as a series combination of the absorption material plus the perforated panel.

To compare this with the experiment results, a simulation is performed to yield the IL of a silencer. The boundary conditions are set as shown in Fig. 7 to obtain SPL from the simulation. Additionally, and denote the sound power level calculated at the end of the duct as shown in Fig. 7(a) and Fig. 7(b), respectively.

(a) Duct with silencer

(b) Duct without silencer

Fig. 7. Boundary conditions for silencer analysis.

3.3 Results

A parametric study is performed to investigate the effects of different sizes of a silencer. Details on the silencer properties are selected based on standards suggested by NORSOK [9], and the same properties are used for all sizes changes for purposes of consistence. The parameters are expressed in Table 2. By using these properties, absorption coefficients are derived with a semi-empirical equation for absorption materials and the acoustic impedance of the perforate panel.

Table 2. Parameters for the experiment and analysis

Parameters		
Absorption material	kind	Mineral wool
	Flow resistivity	2000 $pa \cdot s/m^2$
	Thickness	0.1 m
Perforated panel	Thickness	0.0016 m
	Porosity	0.24
	Hole diameter	0.003 m

The analysis is performed for rectangular silencers with width and height 0.2, 0.3, 0.4, and 0.5 m with unit length (1m) to confirm the effect of the silencer on different large sizes. The comparison is performed for frequencies in the range of 63 – 8000 Hz.

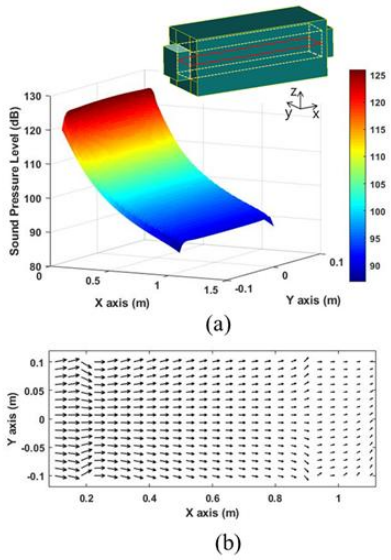

Fig. 8. Energy density level (a) and energy transfer path (b) for the silencers

Fig. 8 indicates the spatial distribution of the acoustic energy density and energy transfer path in the case of the silencer with 0.2 m width at 1000 Hz. Each parameter is shown for the position range from the point where the silencer starts to the point where the silencer ends at 0.5 L on the Z axis. The investigation of the section indicates the total variation in the energy variables in a silencer and the response prediction of the noise source from the inlet. In Fig. 8(a), it is observed that the acoustic energy is dissipated when acoustic waves pass through the absorption material as expected. With respect to the energy transfer path as shown in Fig. 8(b), the acoustic energy flowing from the duct inlet gradually decreases toward the outlet of the duct.

The measurement and analysis results for insertion loss are compared. In Fig. 9, the black lines and red lines indicate the measurement and analysis results, respectively. For the rectangular silencers with widths ranging from 0.2 m to 0.5 m, the comparison between the measurement and the analysis results is performed, and the results indicate reasonably good agreement only within a maximum difference of 4 dB, as shown in Fig. 9. The silencer performance increases steadily to a certain frequency and then decreases again, and thus it is observed that the sound absorption characteristics of the sound absorbing material and perforated panel are well reflected. Furthermore, the results reveal that the peak frequency gradually shifts to higher frequencies when the size increases. The insertion loss decreases when the cross-sectional area of the silencers increases above a specific width, and this implies that the acoustic waves passing through a silencer exhibit a lower probability of meeting absorption materials when the cross-sectional area reaches a specific value. The results indicate that that EFBEM predicts large silencers with widths ranging from 0.2 m to 0.5 m over the mid – high frequency ranges that are not estimated with other methods such as theoretical analysis, namely FEM and BEM.

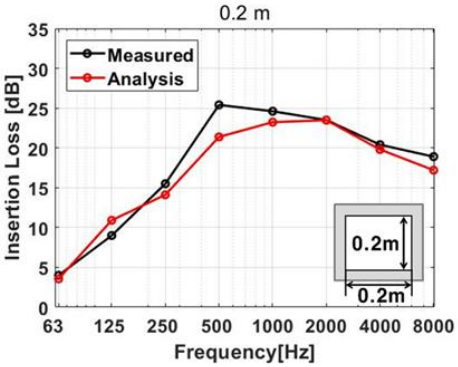

(a) Silencer with a width of 0.2

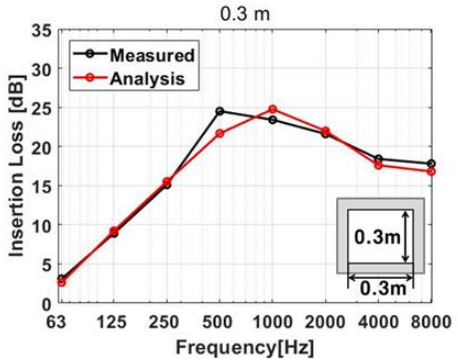

(b) Silencer with a width of 0.3

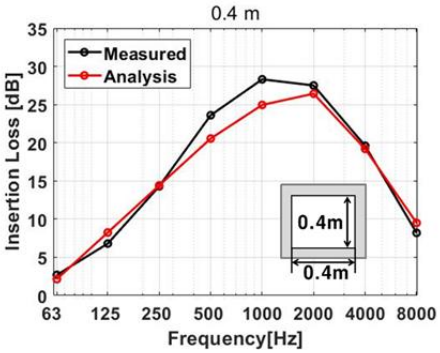

(c) Silencer with a width of 0.4

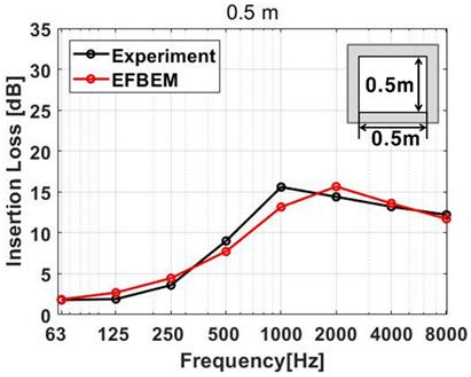

(d) Silencer with a width of 0.5

Fig. 9. Comparison of multi-domain EFBEM and measurement results (air + mineral wool).

4. Conclusions

This study presented an EFA combined with the multi-domain boundary element method to predict the performance of silencers. The surface boundary integral equations are solved by evaluating hypersingular integrals and using the energy density and intensity relation at interfaces between air and the absorption material. Furthermore, the experiment is performed for large silencers to confirm the applicability of EFBEM to large silencers over the mid - high frequency ranges.

The analysis confirms the energy density and energy transfer path. This aids in understanding the mechanism of acoustic energy reduction in a silencer. Additionally, measurement and analysis results are compared for rectangular silencers with widths of 0.2, 0.3, 0.4, and 0.5 m. It is observed that the multi-domain EFBEM results are in reasonably good agreement with the measured data. The results suggest that the approach predicts the performance of the silencers with a relatively low computational cost irrespective of the shape of silencers although the silencer sizes increases. The method is potentially very useful for the prediction of large silencers in the first stage of the design. In ships and offshore plants, there are various spaces such as engine rooms and production·storage facilities as well as residences. Therefore, the HVAC of ships and offshore plants also should analyze the silencer performance based on the flow and temperature effects. Future studies on the development of energy flow model are recommended to reflect these effects.

Acknowledgements

This study was financialy supported by Chonnam National University (Grant number: 2018-3350).

References

[1] Belov, V. D. and S. A. Rybak(1977), Propagation of vibrational energy in absorbing structures, J. Soviet Pysics Acoustic, Vol. 23, pp. 115-119.

[2] Besset, S., M. N. Ichochou, and L. Jézéquel(2010), A coupled BEM and energy flow method for mid-high frequency internal acoustic, Journal of Computational Acoustics, Vol. 18, pp. 69-85.

[3] Bitsie, F.(1996), The structural-acoustic energy finite energy method and energy boundary element method, Purdue University, Doctoral dissertation.

[4] Bride, W. T. and W. D. Bevirt(1994), Sound and vibration design and analysis, 1st Edition, Rockville, Maryland.

[5] Delany, M. E. and E. N. Bazley(1970), Acoustical properties of fibrous materials, Applied acoustics, Vol. 3, No. 2, pp. 105-116.

[6] Errico, F., M. Ichchou, F. Franco, S. De Rosa, O. Bareille, and C. Droz(2019), Schemes for the sound transmission of flat, curved and axisymmetric structures excited by aero dynamic and acoustic sources, Journal of Sound and Vibration, Vol. 456, pp. 221-238.

[7] European Standard EN ISO 29053:1993(1993), Acoustics: materials for acoustical applications. Determination of airflow resistance.

[8] European Standard EN ISO 7235(2003), Measurement procedures for ducted silencers - insertion loss, flow noise and total pressure loss.

[9] Ge, Y. S. and H. B. Zhang(2006), An analysis on 3D acoustic

performance of automotive exhaust muffler, Automotive Engineering, Vol. 28, No. 1, pp. 51-55.

[10] Holland, C. G. and S. F. Wong(1995), Noise prediction and correlation with full scale measurements in ships, Trans IMarE, Vol. 107, No. 3, pp. 195-207.

[11] Ju, H. D., S. B. Lee, and Y. B. Park(2007), Transmission loss estimation of splitter silencer using multi-domain BEM, Journal of Mechanical Science and Technology, Vol. 21, No. 12, pp. 2073-2081.

[12] Kakoty, S. K. and V. K. Roy(2002), Bulk reaction modeling of ducts with and without mean flow, Journal of the Acoustical Society of America, Vol. 112, No. 75, pp. 75-112.

[13] Kirby, R. and A. Cummings(1998), The impedance of perforated plates subjected to grazing gas flow and backed by porous media, Journal of Sound and Vibration, Vol. 217, No. 4, pp. 619-636.

[14] Kirby, R. and P. T. Williams(2014a), A three dimensional investigation into the acoustic performance of dissipative splitter silencers, Journal of the Acoustical Society of America, Vol. 135, No.5, pp. 2727-2737.

[15] Kirby, R. and P. T. Williams(2014b), The effect of higher order modes on the performance of large diameter dissipative silencers, Journal of the Acoustical Society of America, Proceedings of Forum Acusticum.

[16] Ko, S. H(1975). Theoretical analyses of sound attenuation in acoustically lined flow ducts separated by porous splitters (rectangular, annular and circular ducts), Journal of Sound and Vibration, Vol. 39, No. 4, pp. 471-487.

[17] Krishnasamy, G., F. J. Rizzo, L. W. Schmerr, and T. J Rudolphi(1990), Hypersingular boundary integral equations: some applications in acoustic and elastic wave scattering, Journal of applied mechanics, Vol. 27, No. 2, pp. 404-414.

[18] Kwon, H. W., S. Y. Hong, D. H. Park, H. G. Kil, and J. H. Song(2012), Vibrational energy flow models for out-of-plane waves in finite thin shell, Journal of Mechanical Science and Technology, Vol. 26 No. 3, pp. 689-701.

[19] Kwon, H. W., S. Y. Hong, H. W. Lee, and J. H. Song(2011), Power flow boundary element analysis for multi-domain problems in vibrational built-up structures, Journal of sound and Vibration, Vol. 330, pp. 6482-6494.

[20] Lyon, R. H. and R. G. Dejong(1995), Theory and Application of Statistical Energy Analysis, 2nd Edition, Butterworth -Heinemann, London.

[21] Mehdizadeh, O. Z. and M. Paraschivoiu(2005), A three -dimensional finite element approach for predicting the transmission loss in mufflers and silencers with no mean flow, Applied Acoustics, Vol. 66, No. 8, pp. 902-918.

[22] Nefske, D. J. and S. H. Sung(1989), Power flow finite element analysis of dynamic systems: basic theory and application to beams, Journal of Vibration, Acoustics, Stress and Reliability in Design, Vol. 111, No. 1, pp. 94-100.

[23] NORSOK STANDARD(1999), Piping and equipment insulation, R-004, Rev. 2.

[24] Reynolds, D. D. and J. M. Bledsoe(1991), Algorithms for HVAC acoustics, American Society of Heating, Refrigeration and Air Conditioning, Atlanta.

[25] Selamet, A., I. J. Lee, Z. L. Ji, and N. T. Huff(2001), Acoustic attenuation performance of perforated absorbing silencers, SAE Technical Paper 2001-01-1435.

[26] Shojaeefard, M. H. and R. Talebitooti(2012), A study of intake system noise transmission with porous insulator using Statistical Energy Analysis, International Journal of Automotive Engineering, Vol. 2, No, 1.

[27] Soares, C. G. and W. Fricke(2011), Advances in Marine Structure, Boca Raton.

[28] Vérin, O. and N. Fremion(2010), Noise Control: From initial design to launch of the vessel, 10ème Congrès Français d'Acoustique: Lyon, 12-16 April.

[29] Wang, P. and T. W. Wu(2016), Impedance-to-scattering matrix method for large silencer analysis using direct collocation, Engineering Analysis with Boundary Element, Vol. 73, pp. 191-199.

[30] Williams, P. T., R. Kirby, C. Malecki, and J. Hill(2014), Measurement of the bulk acoustic properties of fibrous materials at high temperatures, Applied acoustics, Vol. 77, pp. 29-36.

[31] Williams, P., R. Kirby, J. Hill, M. Abom, and C. Malecki(2018), Reducing low frequency tonal noise in large ducts using a hybrid reactive- dissipative silencer, Applied acoustics, Vol. 131, pp. 61-69.

[32] Wu, T. W.(1998), A direct boundary element method for acoustic radiation and scattering from mixed regular and thin bodies, Journal of the Acoustical Society of America, Vol. 97, No. 1, pp. 767-779.

[33] Wu, T. W. and G. C. Wan(1996), Muffler performance studies using a direct mixed-body boundary element method and a three-point method for evaluating transmission loss, Journal of Sound and Vibration, Vol. 118, No. 3, pp. 479-484.

[34] Yao, D., J. Zhang, R. Wang, X. Xiao, and J. Guo(2019), Lightweight design and sound insulation characteristic optimisation of railway floating floor structures, Applied Acoustics. Vol. 156, pp. 66-77.

Received : 2020. 05. 11.
Revised : 2020. 05. 22.
Accepted : 2020. 05. 28.